Theoretical 13 C NMR spectra of IPR isomers of fullerene C 80: a density functional theory study

ARTICLE *in* CHEMICAL PHYSICS LETTERS · OCTOBER 2000

Impact Factor: 1.9 · DOI: 10.1016/S0009-2614(00)00969-6

2 AUTHORS:

Guangyu Sun
Pennsylvania State University
56 PUBLICATIONS **1,293** CITATIONS
SEE PROFILE

Miklos Kertesz
Georgetown University
226 PUBLICATIONS **6,580** CITATIONS
SEE PROFILE

6 October 2000

ELSEVIER

Chemical Physics Letters 328 (2000) 387–395

CHEMICAL PHYSICS LETTERS

www.elsevier.nl/locate/cplett

Theoretical ^{13}C NMR spectra of IPR isomers of fullerene C_{80}: a density functional theory study

Guangyu Sun, Miklos Kertesz *

Department of Chemistry, Georgetown University, 606 Reiss Building, 37th and O Streets, NW, Washington DC 20057-1227, USA

Received 17 July 2000

Abstract

Optimized geometries and ^{13}C NMR chemical shifts of fullerene C_{80} have been calculated by density functional theory using B3LYP/6-31G* for all isolated-pentagon-rule isomers with non-zero HOMO–LOMO gap (isomers **1**, **2**, **3**, **4** and **5**). D_2 distorted isomer **7** is predicted as first-order saddle-point by B3LYP/STO-3G. The calculated NMR spectrum of isomer **2** agrees well with experiment of Hennrich, confirming the assignment unequivocally. The predicted spectra of other isomers either show unusually large spectral span or have unusual chemical shifts for some sites, indicating unfavorable electron distribution. Both energetic and NMR properties indicate these isomers are less stable than isomer **2**. © 2000 Elsevier Science B.V.

1. Introduction

The synthesis, separation and identification of extractable isomers of higher fullerenes have drawn constant interest since the first fullerene, C_{60}, was discovered [1] in 1985 and identified by IR [2] and NMR [3] in 1990. HPLC and NMR techniques are the most powerful separating and identifying tools in this sense. As a result, a number of isomers of various higher fullerenes have been characterized by NMR, including one isomer of C_{70} [3,4], one isomer of C_{76} [5], three isomers of C_{78} [6–8], one isomer of C_{80} [9] and four isomers of C_{84} [10,11]. Three isomers of C_{82} [7], several minor isomers of C_{84} [12] and one high symmetry isomer of C_{90} [8] also exist, although their separation and identification has not been achieved experimentally.

All carbon atoms in fullerene are sp^2 hybridized. Resulting from the cage-like geometry and the sp^2 hybridization of carbon atom, the minimization of steric strain and maximization of π-electron delocalization leads to the isolated-pentagon-rule (IPR) [13], which states that the most stable isomers have structures with all pentagons isolated from each other. This rule dramatically reduces the number of likely isomers. It is, however, still quite common that a fullerene has more than one IPR isomers having the same symmetry, which is likely to give similar NMR chemical shift patterns. For example, four IPR isomers of C_{84} have D_2 symmetry and all have 21 NMR peaks with equal intensity. In case these isomers have similar total energies, the identification could be facilitated by quantitative theoretical NMR patterns.

Theoretical studies on NMR patterns of fullerenes have gained more and more interest recently.

* Corresponding author. Fax: +1-202-687-6209.
E-mail address: kertesz@georgetown.edu (M. Kertesz).

0009-2614/00/$ - see front matter © 2000 Elsevier Science B.V.
PII: S0009-2614(00)00969-6

The chemical shifts of C_{60} and C_{70} with respect to that of benzene were calculated at the GIAO–CPHF/DZP level (Gauge-independent atomic orbital–coupled-perturbed Hartree–Fock) [14]. NMR chemical shift predictions for C_{70} were used to help selecting the best model for interpreting gas-phase electron diffraction (GED) experiments [15]. Hartree–Fock (HF) and density functional theory (DFT) methods were employed to accurately calculate the chemical shifts of C_{60} and C_{70} [16]. Calculated spectral spans were used to rule out the D_2 distorted I_h isomer, $D_2(I_h)$, of C_{80} as the experimentally observed isomer [9]. For fullerene C_{84}, isomers **1** and **5** (numbering after Manolopoulos and Fowler [17], their numbering will be used throughout this paper) were eliminated as the candidate for the observed D_2 isomer by comparing the calculated spans of the NMR spectra with the experimental values [18]. In a recent study by Heine et al. [19], chemical shifts of C_{70}, C_{76}, C_{78}, $(C_{36})_2$, $(C_{60})_2$ and several isomers of C_{84} were calculated using the individual gauge for local orbitals–density functional based tight-binding (IGLO–DFTB) method. Based on the spectral span and total energy, their calculations support the assignment of the two major isomers of C_{84}. A later report [20] describes the NMR patterns of all IPR isomers of fullerenes C_{84}. We have recently [21] utilized the B3LYP functional in combination with the 6-31G* and 6-311G** basis sets to predict the NMR spectra of isomers **21**, **22** and **23** of C_{84}. The small rms values (less than 0.6 ppm) of our predicted NMR peaks for isomers **22** and **23** allowed us for the first time based solely on NMR evidence to confirm that isomers **22** and **23** are the experimentally obtained major isomers. B3LYP/6-31G* also proved to be sufficiently accurate [22] in reproducing ^{13}C NMR chemical shifts of fullerenes C_{60}, C_{70}, C_{76} and C_{78}.

As a part of our continued effort, the NMR chemical shifts of fullerene C_{80} are studied here. The main goals of this work are to reproduce the NMR chemical shifts of C_{80} to confirm the isomer assignment as well as to show the good performance of density functional theory on the NMR properties of fullerenes thus validating this approach for studying other higher fullerenes. For the seven possible IPR isomers of fullerene C_{80}, Hückel treatment showed that the D_{5h} and I_h isomers have open-shell electronic configurations and the other five isomers are closed-shell systems [13]. The five closed-shell isomers, namely isomers **1**, **2**, **3**, **4** and **5**, were studied in this work. Since the I_h isomer could distort to D_2 symmetry due to the Jahn–Teller effect and a D_2 isomer was observed in experiment, the D_2 distorted isomer **7** was also considered in this work. Fig. 1 shows the six isomers of fullerene C_{80} studied. Geometries of these isomers were optimized using B3LYP functional and various basis sets. ^{13}C NMR chemical shielding tensors were then evaluated using the 6-31G* and 6-311G** basis sets. NMR chemical shifts of isomer **2** are compared with experiment while chemical shifts of other isomers were used to provide clues for their stability.

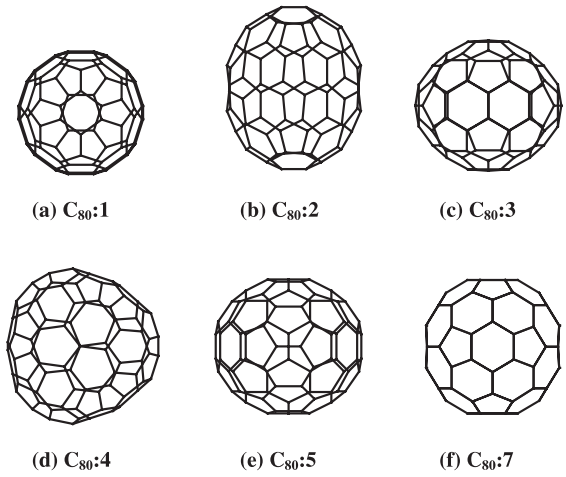

Fig. 1. Six IPR isomers of fullerence C_{80} that are studied in this work. Isomer numbering is according to Ref. [13].

2. Computational details

Full geometry optimizations and NMR chemical shielding calculations were performed for all five IPR isomers of fullerene C_{80}, isomers **1**, **2**, **3**, **4** and **5**, with non-zero HOMO–LOMO gap as well as a D_2 distorted form of isomer **7**, $D_2(I_h)$. Becke's three-parameter (B3) hybrid functional [23] incorporating exact exchange in combination with Lee, Yang and Parr's (LYP) correlation functional

[24] was used throughout this study. First, geometry optimizations were performed using the minimum basis set, STO-3G. To ensure the optimized geometries are indeed minima, vibrational analyses were carried out for all isomers at the B3LYP/STO-3G level of theory. The optimized geometry of the D_2 form of isomer **7** distorts from I_h symmetry only slightly and turns out to be a first-order saddle point. The displacement vector corresponding to the imaginary frequency leads to an even lower symmetry structure and, therefore, this isomer was not included in subsequent calculations. The geometries of isomers **1**, **2**, **3**, **4**, and **5** correspond to real minima and were further optimized using the 3-21G and 6-31G* basis sets. NMR chemical shielding tensors were evaluated employing the GIAO method [25] at the B3LYP/6-31G* optimized geometry. The 6-31G* and 6-311G** basis sets were used upon the recommendation by Cheeseman et al. [26] and based on our own experience [21,22]. For isomer **2**, additional geometry optimization and NMR calculation were performed using the 6-31G basis set. Gaussian 98 [27] was used for geometry optimizations and the vibrational analyses while the PQS suite of ab initio programs [28] were used for NMR calculations.

The following formula was then used to calculate the chemical shift (δ) from the calculated chemical shielding (σ) for carbon atom i by referencing to that of C_{60} at any given level of theory:

$$\delta(i) = \delta(C_{60}) + \sigma(C_{60}) - \sigma(i), \quad (1)$$

where $\delta(C_{60})$ is taken as 143.15 ppm, after Avent et al. [12]. The values of calculated chemical shielding of C_{60}, $\sigma(C_{60})$, are 51.81, 50.59 and 32.70 ppm using the 6-31G, 6-31G* and 6-311G** basis sets, respectively.

3. Results and discussion

3.1. Energy and geometry

Several earlier theoretical studies have addressed the stability of the isomers of C_{80} and, sometimes, conflicting results were obtained. A tight-binding molecular-dynamics (TBMD) study on C_{80} predicted [29] a distorted form of isomer **6**, $C_s(D_{5h})$, having the lowest energy. Single point energy calculations [30] carried out using generalized-gradient approximation (GGA) at the non-self-consistent-field (non-SCF)-MO optimized geometry predicted the D_2 isomer to have relatively low energy and the largest HOMO–LUMO gap, thus most probably to be observed experimentally. Calculations using semi-empirical AM1 and SAM1 methods showed [31] the D_{5d} isomer as the most stable one, and the D_2 isomer to be 5.26 kcal/mol less stable. Subsequent ab initio single-point calculations showed the same trend [32]. Quantum consistent force field for π-electrons (QCFF/PI) predicted [33] that isomers **1** and **2** have the lowest energies. Using HF and several DFT approximations along with the 3-21G basis set, single point calculations [34] performed at the AM1 optimized geometries predicted that isomers D_2 and $D_5(D_{5d})$ are essentially isoenergetic.

The statistics of bond lengths and HOMO–LUMO gaps calculated by B3LYP/6-31G* and relative energies obtained by various levels of theory are listed in Table 1 for all C_{80} isomers studied in this Letter. Also listed are the relative energies of C_{80} isomers as obtained by earlier theoretical studies [29–31,33,34]. Isomer **7** is only studied using B3LYP/STO-3G. All calculated bond lengths are within the 1.36–1.48 Å range. The average bond lengths are even more similar, varying only from 1.432 to 1.433 Å. The geometrical features are essentially the same to that of earlier cases [22].

From the most to least stable, the order of stability of the five isomers at the B3LYP/6-31G* level is: **2** > **1**–**3** > **5**–**4**. When smaller basis sets are used, this order essentially remains although the absolute values of energies change by as much as 8 kcal/mol for isomer **5**. Some earlier theoretical results obtained by either the AM1 semi-empirical method [31] or by HF single point energy at the AM1 optimized geometry [34] generally agree with the current findings. Other results by TBMD [29] and GGA//non-SCF [30] methods show large discrepancies. It appears that our results, which are at the highest level of theory applied so far to these isomers, give a consistent picture both in terms of

Table 1
Bond length statistics and relative energies of IPR isomers of fullerene C_{80} calculated by DFT[a]

	$C_{80}:1$ D_{5d}	$C_{80}:2$ D_2	$C_{80}:3$ C_{2v}	$C_{80}:4$ D_3	$C_{80}:5$ C_{2v}	$C_{80}:7$ $D_2(I_h)$
Shortest R_{cc}[b]	1.393	1.379	1.367	1.382	1.365	
Longest R_{cc}^b	1.468	1.469	1.474	1.467	1.476	
Average R_{cc}^b	1.4330	1.4329	1.4326	1.4327	1.4326	
B3LYP/STO-3G	0.64	0.00	7.60	10.95	12.52	38.83[c]
B3LYP/3-21G	0.16	0.00	8.75	11.54	14.62	
B3LYP/6-31G*	2.20	0.00	2.80	8.89	6.61	
$\Delta E_{HOMO-LUMO}$[d]	0.986	1.346	0.868	0.743	0.708	
TBMD[e]	−1.73	0.00	−1.38	3.23	1.73	6.71
GGA//non-SCF[f]	73.8	0.00	−18.4	36.9	0.0	−36.9
AM1[g]	−5.26	0.00	13.16	27.51	21.05	66.75
PCFF/PI[h]	0.3	0.00	2.7	18.1	7.0	34.4
HF//AM1[i]	−2.3	0.00	21.3	33.7	36.2	99.7

[a] Bond lengths in Å, energy in kcal/mol.
[b] Bond length statistics of B3LYP/6-31G* geometries.
[c] First-order saddle point indicated by vibrational analysis by B3LYP/STO-3G.
[d] HOMO–LUMO gap (in eV) calculated by B3LYP/6-31G*, this Letter.
[e] Taken from Ref. [29].
[f] Taken from Ref. [30].
[g] Taken from Ref. [31].
[h] Taken from Ref. [33].
[i] Taken from Ref. [34].

energetic, and as we will discuss, in terms of NMR chemical shifts.

The HOMO–LUMO gap of isomer **2** is predicted to be 1.346 eV. This value is lower by 0.27 eV than the HOMO–LUMO gap of $C_{78}:1$, which has the lowest HOMO–LUMO gap among the stable fullerenes, C_{60}, C_{70}, $C_{76}:1$, $C_{78}:1$, $C_{78}:2$ and $C_{78}:3$, calculated at the same level of theory [22]. On the other hand, it is higher than those of the unobserved isomers of C_{80} by at least 0.36 eV. Thus the energetic and electronic properties both indicate that isomer **2** is the most stable isomer among the IPR isomers of C_{80}.

3.2. NMR chemical shifts

Experimental NMR spectrum of fullerene C_{80} shows 20 peaks with equal intensities. Two isomers, isomer **2** and the D_2 distorted form of isomer **7**, should give such NMR patterns. Based on the calculated spans of NMR spectra, the $D_2(I_h)$ isomer was ruled out and isomer **2** was assigned to be the experimentally obtained isomer by Hennrich et al. [9]. By comparing the theoretical and experimental NMR spectra of isomer **2** in detail, we confirm this assignment. As mentioned above, the $D_2(I_h)$ isomer turns out to be a first-order saddle point at the B3LYP/STO-3G level of theory and NMR calculation was not performed for isomer **7**. The theoretical NMR spectra of other isomers will also be described.

The calculated NMR chemical shifts of isomers **1**, **2**, **3**, **4** and **5** are listed in Table 2. The predicted chemical shifts by B3LYP/6-31G* are listed in numerical order. Other chemical shifts are listed in such a way that, for the each row, the corresponding carbon atoms are the same to the one in the B3LYP/6-31G* column. Carbon atom types are assigned to pyracylene, corannulene and pyrene type, following Diederich et al. [6].

We discuss the results of isomer **2** the first since it is the experimentally obtained one. This isomer has D_2 symmetry thus has 20 NMR peaks with equal intensity. The calculated NMR spectra, in general, agree with the experimental spectrum (see Fig. 2). The experimentally measured spectral span is 23.6 ppm. The experimental spectrum shows three groups, each containing 3, 6 and 11 peaks

Table 2
^{13}C NMR chemical shifts of IPR isomers of C_{80} calculated at the B3LYP/6-31G* optimized geometry[a]

C_{80} : **1**			C_{80} : **2**					C_{80} : **3**			C_{80} : **4**			C_{80} : **5**		
B3LYP/ 6-31G*	B3LYP/ 6-311G**	Type[b]	Exp.[c]	B3LYP/ 6-31G*	B3LYP/ 6-311G**	B3LYP/ 6-31G[d]	Type[b]	B3LYP/ 6-31G*	B3LYP/ 6-311G**	Type[b]	B3LYP/ 6-31G*	B3LYP/ 6-311G**	Type[b]	B3LYP/ 6-31G*	B3LYP/ 6-311G**	Type[b]
159.59[e]	161.05[e]	pc	152.9	153.26	154.24	152.95	pc	166.89	168.29	pc	163.89	165.62	cor	157.48	157.83	cor
154.66[e]	155.81[e]	pc	152.6	152.75	153.73	152.71	pc	158.19	159.03	pc	160.83	162.64	cor	151.99	152.10	cor
146.98	147.85	pc	151.4	151.33	152.01	151.69	pc	150.37[e]	150.97[e]	pc	159.74	160.92	cor	151.47[e]	150.16[e]	py
135.28	134.49	py	146.1	145.31	145.81	145.97	pc	149.05	149.33	cor	153.96	154.45	cor	149.91	149.99	cor
94.39	89.06	cor	144.4	144.22	144.53	144.67	pc	148.79	149.32	cor	148.21	150.02	pc	149.01	148.83	pc
			144.4	143.76	144.09	143.99	pc	148.54[e]	148.74[e]	cor	147.39	148.91	pc	147.91[e]	148.21[e]	pc
			143.8	143.42	143.84	144.57	pc	143.44	143.84	pc	142.68	142.69	py	142.69[e]	143.52[e]	cor
			142.8	142.55	142.69	143.82	pc	143.17	143.08	cor	139.41[f]	138.32[f]	py	141.52	141.90	pc
			142.6	140.97	141.18	142.20	pc	142.34	142.34	cor	137.99	137.59	py	139.90	139.98	cor
			138.9	140.76	140.21	140.10	py	141.56	141.86	pc	137.89	137.65	cor	139.53	138.55	py
			138.7	139.82	139.25	138.90	py	141.44[e]	141.76[e]	pc	137.88	137.80	py	139.33	139.30	cor
			138.1	137.97	137.71	139.41	cor	139.00	139.03	cor	137.33	138.01	pc	136.44	136.73	pc
			137.1	136.83	136.21	136.21	py	138.32	138.52	pc	135.63	135.73	pc	135.94[e]	135.81[e]	py
			136.9	136.03	135.69	136.90	cor	137.05	136.44	py	131.05	129.68	pc	135.91	135.43	py
			136.1	135.84	135.41	137.72	cor	135.77	134.94	py				135.72	134.78	py
			135.3	134.42	133.96	135.61	cor	134.78	133.83	py				133.85	133.80	py
			134.2	133.50	132.67	133.45	py	134.63	134.25	cor				132.30	131.37	cor
			133.0	132.11	130.86	132.04	py	134.50	134.19	py				130.69	130.49	cor
			131.1	131.81	131.02	133.64	cor	133.70[e]	133.71[e]	pc				125.43	125.41	pc
			129.3	126.07	124.82	128.35	cor	132.07[e]	131.65[e]	py				122.98	122.69	cor
								130.37[e]	129.54[e]	py				116.53	115.42	cor
								118.48	117.77	cor				112.24	111.47	cor
								116.52	115.69	cor						

[a] Chemical shifts, in ppm, are referenced to that of C_{60} at 143.15 ppm.
[b] pc – pyracylene; cor – corannulene; py – pyrene.
[c] Experimental values taken from Ref. [9].
[d] Calculated at the B3LYP/6-31G optimized geometry.
[e] Half intensity peaks.
[f] The peak of C_{80} : 4 with 1/3 of full intensity.

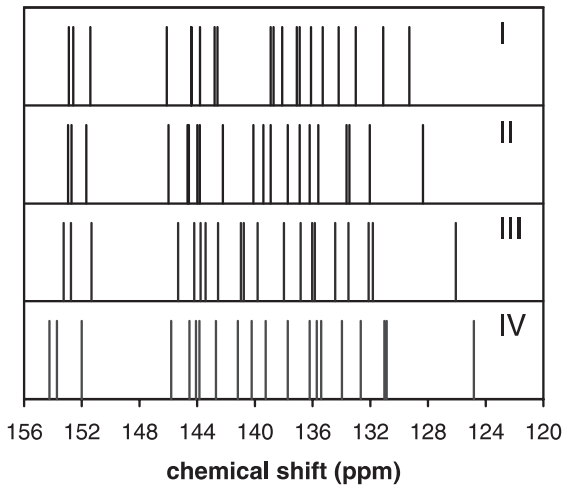

Fig. 2. ^{13}C NMR spectra of isomer **2** of C_{80} by (I) experiment [9], (II) B3LYP/6-31G, (III) B3LYP/6-31G*, (IV) B3LYP/6-311G**. All spectra are referenced to C_{60} at 143.15 ppm.

from downfield to upfield. We note that the second group appears to have only five peaks since two peaks accidentally have identical values of chemical shift. The first group is separated from the second group by a larger distance than that between the second and the third groups. The calculated spectral spans are 24.60, 27.19 and 29.42 ppm by 6-31G, 6-31G* and 6-311G**, respectively. All three calculated spectra show a distinct group of three peaks in the 150–154 ppm range. Since the low symmetry of higher fullerene isomers makes the number of their NMR peaks very large, we expect that the groupings of a certain number of peaks, besides the spectral span, acts as the decisive evidence for fullerene identification. The 6-31G spectrum shows the two other groups, although the separation between them is not as wide as in the experiment. The spectra predicted by the 6-31G* and 6-311G* basis sets fail to separate these two groups and all the remaining 17 peaks spread over the 124–146 ppm range. This comparison fits the general trend [22], where peaks above 140 ppm are better reproduced than peaks below 140 ppm. The performance of 6-31G on isomer **2** is as good as that of 6-31G** for earlier cases of C_{70}, C_{76}, C_{78} and C_{84}, while the performance of 6-31G* and 6-311G** is comparable to that of 6-31G* on $C_{78}:3$ where the agreement between theoretical and experimental results is the worst among isomers for which experimental results are available [22]. The inclusion of polarization function in the basis set of carbon atom does not seem to enhance the performance of the basis set. As in the earlier cases [21,22], we do not attempt one-to-one assignment for NMR peaks due to the crowdedness of the peaks in the spectrum.

The predicted NMR spectra of the unobserved isomers are compiled in Fig. 3. Isomer **1** has D_{5d} symmetry and shows three full-intensity peaks and two half-intensity peaks. Our predictions give two full-intensity peaks and two half-intensity peaks in the range of 130–160 ppm where the fullerene NMR peaks usually appear. The other full-intensity peak, however, is predicted to occur at around 90 ppm. This is close to the region in which sp^3 carbons in fullerenes normally appear, for example, in $(C_{60})_2$ [35]. This peak corresponds to the fourth distinct site from cap to equator. It has been suggested that the wide spread of chemical shifts of a fullerene might be related to uneven charge distribution within the molecule [9]. The charge on these sites is predicted to be -0.033 by Mulliken population analysis at the B3LYP/6-31G* level of theory. This kind of charge is not unusual in the observed fullerene isomers. For instance in the case of isomer **2**, the charges are 0.051 and -0.034 for carbon atoms corresponding to the NMR peaks at 140.76 and 126.07 ppm, respectively. Thus, the idea of uneven charge distribution does not explain this unusual chemical shift. It seems to be the electron distribution resulted from the unique topology of a given isomer that gives rise to the NMR pattern.

Isomer **3** of C_{80} has C_{2v} symmetry and shows 17 full-intensity peaks and six half-intensity peaks. The calculated NMR peaks occur between 110 and 170 ppm, which is larger than normal spans of fullerenes. Five groups each containing 1, 1, 2, 11 and 2 full-intensity peaks exist from downfield to upfield in the predicted spectra. The half-intensity peaks occur in the 130–151 ppm range and form three groups containing 2, 1 and 3 peaks from downfield to upfield.

Isomer **4** has D_3 symmetry and shows 13 full-intensity peaks plus one peak with 1/3 intensity.

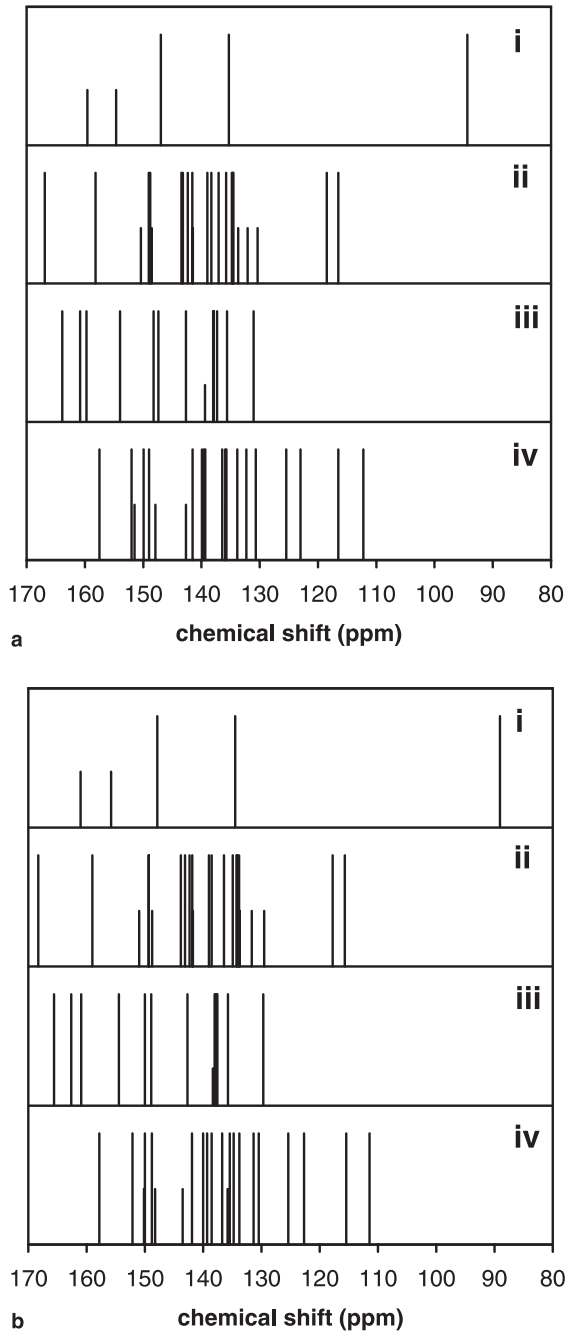

Fig. 3. Calculated ^{13}C NMR spectra of C_{80} by (a) B3LYP/6-31G* and (b) B3LYP/6-311G** of (i) isomer **1**, (ii) isomer **3** (iii) isomer **4** and (iv) isomer **5**. All spectra are referenced to C_{60} at 143.15 ppm.

The predicted NMR peaks occur within the normal range of fullerene NMR spectra. The spectral span of isomer **4** resembles those of the observed fullerenes most closely among the unobserved isomers of C_{80}. The 13 full-intensity peak spread over the whole range and grouping of peaks is not apparent. The 1/3 intensity peak appears at about 139 ppm.

Isomer **5** has C_{2v} symmetry and shows 18 full intensity peaks and four half-intensity peaks. The span of the calculated NMR spectra is similar to that of isomer **3**. Similarly to the case of isomer **4**, the full-intensity peaks occur within the whole range of the spectrum and no grouping of peaks is apparent. The four half-intensity peaks occur in the range of 136–152 ppm.

3.3. Chemical shifts and connectivity

The local connectivity has been suggested to have influence on the chemical shift in fullerenes [5,6]. Three types of carbon sites in fullerenes were used to categorize the carbon atoms and to help to assign the experimental NMR peaks: pyracylene site (type 1, pc), corannulene site (type 2, cor) and pyrene site (type 3, py). The chemical shifts of these sites should appear in the pc > cor > py order. Later theoretical works [19,22] utilized this concept to correlate the local connectivity and chemical shifts. At the B3LYP/6-31G* level of theory, the range of chemical shifts are 133–152 ppm for type 1 sites, 136–148 ppm for type 2 sites and 130–142 ppm for type 3 sites for observed isomers of fullerenes C_{70}, C_{76}, C_{78} and C_{84} [22].

The type of the carbon site of C_{80} isomers is given for all NMR peaks in Table 2. For isomer **2**, type 1 sites have higher values of chemical shifts than type 2 and type 3 sites, while the chemical shifts of the latter two types are mixed. For isomer **1**, the peak at 90 ppm is far away from the normal range of type 2 sites. For the isomers **3**, **4** and **5**, the calculated chemical shifts of different sites deviate significantly from the pc > cor > py order. This indicates that the electron distribution in these isomers is less optimal and thus these isomers are unstable. For instance, among the unobserved isomers, isomer **4** has normal span of

NMR spectrum. However, in addition to its relatively high energy, the chemical shifts of type 2 carbon atoms have chemical shifts as high as 163.89 ppm by B3LYP/6-31G*, which is much above the upper boundary of the normal range of type 2 sites, 148 ppm [22]. Therefore, the high relative energy, the low HOMO–LUMO gap and the abnormal NMR chemical shifts indicate it as an unfavorable candidate to be experimentally obtained.

4. Conclusion

In summary, geometry optimization has been performed on all closed-shell IPR isomers of fullerene C_{80} using density functional theory. Employing the GIAO method, the ^{13}C NMR chemical shifts were evaluated at the B3LYP/6-31G* level of theory. For isomer **2**, the calculated chemical shifts agree with experiment in general. Peaks above 140 ppm appear to agree better with experiment than peaks below 140 ppm. Our calculation confirms the assignment of isomer **2** based on four criteria: (1) good agreement of chemical shifts; (2) lowest total energy among possible isomers; (3) largest HOMO–LUMO gap; and (4) no unusual chemical shifts for any carbon site. For the unobserved isomers, our predictions show unusual NMR behavior. Combined with the calculated relative energy, the unusual NMR behavior indicates the reason why these isomers are unstable.

Acknowledgements

This work is supported by National Science Foundation under Grants CHEM-9802300 and CHEM-9601976 (Georgetown University Molecular Modeling Center).

References

[1] H.W. Kroto, J.R. Heath, S.C. O'Brien, R.F. Curl, R.E. Smalley, Nature 318 (1985) 162.
[2] W. Krätschmer, L.D. Lamb, K. Fostiropoulos, D.R. Huffman, Nature 347 (1990) 354.
[3] R. Taylor, J.P. Hare, A.K. Abdul-Sada, H.W. Kroto, J. Chem. Soc. Chem. Commun. (1990) 1423.
[4] R.D. Johnson, G. Meijer, J.R. Salem, D.S. Bethune, J. Am. Chem. Soc. 113 (1991) 3619.
[5] R. Ettl, I. Chao, F. Diederich, R.L. Whetten, Nature 353 (1991) 149.
[6] F. Diederich, R.L. Whetten, Acc. Chem. Res. 25 (1992) 119.
[7] K. Kikuchi, N. Nakahara, T. Wakabayashi, S. Suzuki, H. Shiromaru, Y. Miyake, K. Saito, I. Ikemoto, M. Kainosho, Y. Achiba, Nature 357 (1992) 142.
[8] R. Taylor, G.J. Langley, A.G. Avent, T.J.S. Dennis, H.W. Kroto, D.R.M. Walton, J. Chem. Soc., Perkin Trans. 2 (1993) 1029.
[9] F.H. Hennrich, R.H. Michel, A. Fischer, S. Richard-Schneider, S. Gilb, M.M. Kappes, D. Fuchs, M. Bürk, K. Kobayashi, S. Nagase, Angew. Chem. Int. Ed. Engl. 35 (1996) 1732.
[10] T.J.S. Dennis, T. Kai, T. Tomiyama, H. Shinohara, Chem. Commun. (1998) 619.
[11] N. Tagmatarchis, A.G. Avent, K. Prassides, T.J.S. Dennis, H. Shinohara, Chem. Commun. (1999) 1023.
[12] A.G. Avent, D. Dubois, A. Pénicaud, R. Taylor, J. Chem. Soc., Perkin Trans. 2 (1997) 1907.
[13] P.W. Fowler, D.E. Manolopoulos, An Atlas of Fullerenes, Oxford University Press, New York, 1995.
[14] M. Häser, R. Ahlrichs, H.P. Baron, P. Weis, H. Horn, Theor. Chim. Acta 83 (1992) 455.
[15] K. Hedberg, L. Hedberg, M. Bühl, D.S. Bethune, C.A. Brown, R.D. Johnson, J. Am. Chem. Soc. 119 (1997) 5314.
[16] M. Bühl, M. Kaupp, O.L. Malkina, V.G. Malkin, J. Comput. Chem. 20 (1999) 91.
[17] D.E. Manolopoulos, P.W. Fowler, J. Chem. Phys. 96 (1992) 7603. Also see the tables in Ref. [13].
[18] U. Schneider, S. Richard, M.M. Kappes, R. Ahlrichs, Chem. Phys. Lett. 210 (1993) 165.
[19] T. Heine, G. Seifert, P.W. Fowler, F. Zerbetto, J. Phys. Chem. A 103 (1999) 8738.
[20] T. Heine, M. Bühl, P.W. Fowler, G. Seifert, Chem. Phys. Lett. 316 (2000) 373.
[21] G. Sun, M. Kertesz, New J. Chem., accepted.
[22] G. Sun, M. Kertesz, J. Phys. Chem. A 104 (2000) 7398.
[23] A.D. Becke, J. Chem. Phys. 98 (1993) 5648.
[24] C. Lee, W. Yang, R.G. Parr, Phys. Rev. B 37 (1988) 785.
[25] K. Wolinski, J.F. Hinton, P. Pulay, J. Am. Chem. Soc. 112 (1990) 8251.
[26] J.R. Cheeseman, G.W. Trucks, T.A. Keith, M.J. Frisch, J. Chem. Phys. 104 (1996) 5497.
[27] Gaussian 98, Revision A.5, M.J. Frisch et al., Gaussian Inc., Pittsburgh PA, 1998.
[28] PQS, version 2.1, Parallel Quantum Solutions, Fayetteville, Arkansas, 1998.
[29] B.L. Zhang, C.Z. Wang, K.M. Ho, C.H. Xu, C.T. Chan, J. Chem. Phys. 98 (1993) 3095.

[30] K. Nakao, N. Kurita, M. Fujita, Phys. Rev. B 49 (1994) 11415.
[31] M.L. Sun, Z. Slanina, S.L. Lee, F. Uhlík, L. Adamowicz, Chem. Phys. Lett. 246 (1995) 66.
[32] Z. Slanina, S.L. Lee, L. Adamowicz, Int. J. Quantum Chem. 63 (1997) 529.
[33] P.W. Fowler, F. Zerbetto, Chem. Phys. Lett. 243 (1995) 36.
[34] K. Kobayashi, S. Nagase, T. Akasaka, Chem. Phys. Lett. 245 (1995) 230.
[35] G.W. Wang, K. Komatsu, Y. Murata, M. Shiro, Nature 387 (1997) 583.